Removal of arsenic from aqueous solution by iron-coated sand and manganese-coated sand having different mineral types

Yoon-Young Chang, Ki-Hoon Song, Mok-Ryun Yu and Jae-Kyu Yang

ABSTRACT

In this study, the effects of the coating temperature during the preparation of manganese-coated sand (MCS) and iron-coated sand (ICS) on the removals of As(III) and As(V) were evaluated. The mineral type of manganese oxide on MCS-150, prepared at 150 °C, was identified as a mixture of pyrolusite and ramsdellite, which changed to high crystalline pyrolusite above 300 °C. The mineral type of ICS-150, prepared at 150 °C, was a mixture of goethite and hematite, which changed to high crystalline goethite above 300 °C. The adsorption efficiency was determined according to the mineral type which depended on the coating temperature. The As(III) oxidation efficiency of MCS-150 and As(V) adsorption efficiency of ICS-150 were approximately 77 and 70% higher compared with those of MCS-600 and ICS-600, respectively, prepared at 600 °C. Regardless of the coating temperature, the amounts of manganese and iron coated on the sand substrates were similar.

Key words | adsorption, arsenic, iron-coated sand, manganese-coated sand, oxidation

Yoon-Young Chang
Ki-Hoon Song
Mok-Ryun Yu
Department of Environmental Engineering,
Kwangwoon University,
Seoul,
Korea

Jae-Kyu Yang (corresponding author)
Division of General Education,
Kwangwoon University,
Seoul,
Korea
E-mail: *jkyang@kw.ac.kr*

INTRODUCTION

Arsenic generally contaminates soil and water systems due to various anthropogenic sources, such as mining activities, discharges of industrial wastes and agricultural application, as well as geochemical reactions (Kim *et al.* 2002; Smedley & Kinniburgh 2002). Although arsenic has multiple oxidation states (+5, +3, 0 and −3), As(III) and As(V) are the main inorganic arsenic species found in soils and sediments. Generally, the preferential oxidation state in sediments or the aqueous phase under anaerobic conditions is known to be As(III). As(III) is much more toxic, soluble and mobile than As(V) (Chen *et al.* 1999).

As the safe and effective treatment of wastewater containing organic compounds, heavy metals, including metalloids, is always a challenging task, many investigations have focused on the development of cost-effective techniques (Srivastava *et al.* 1997; Gupta *et al.* 1997a, b, 1998, 2009, 2010; Gupta & Sharma 2002; Ali & Gupta 2007; Gupta & Ali 2008; Gupta & Rastogi 2008a, b). In order to treat arsenic in water systems, several synthetic Fe-containing adsorbents, such as silica-containing iron oxide, and iron oxide-loaded slag, have been applied (Gupta *et al.* 2005; Zhang & Itoh 2005). However, these processes

are only partially effective for the treatment of As(III) as there is also the need to control the solution pH and/or other parameters to achieve optimal arsenic removal efficiency. Thus, many investigations have focused on the development of simple and cost-effective techniques for the oxidation of As(III). As promising techniques, manganese-coated sand (MCS) and iron-coated sand (ICS) have been applied in the treatment of both As(III) and As(V) (Chang *et al.* 2007, 2008; Yang *et al.* 2007).

In previous studies, ICS coated with hematite and goethite showed significant removal capacities for As(III) and As(V) through adsorption. Also Giménez *et al.* (2007) reported that both As(III) and As(V) were efficiently sorbed onto hematite rather than goethite or magnetite. Although MCS coated with pyrolusite (δ-MnO_2) showed much less adsorption capacity for As(V) than ICS, it showed good As(III) oxidation efficiency (Chang *et al.* 2007). However very limited information is available on the removal efficiencies of arsenic by ICS and MCS and the conditions required for their preparation.

As oxidation and adsorption are important processes for controlling arsenic mobility in subsurface systems as well as

for the treatment of water contaminated with arsenic, the removal efficiencies of both As(III) and As(V) by MCS and ICS prepared at different coating temperatures were investigated in this study.

MATERIALS AND METHODS

Materials

Joomoonjin sand, with a particle size ranging from 1.0 to 1.2 mm and widely used as standard sand in Korea, was used as the supporting material for iron and manganese. Prior to coating of the iron and manganese onto the sand, the raw sand was pre-washed with 0.1 mol/L HCl for 2 h and rinsed three times with deionized water to remove any impurities. All chemicals were of analytical grade. As_2O_3, $FeCl_3$ and $Mn(NO_3)_2$ were purchased from Aldrich Chemicals. The As(III) stock solution was prepared by dissolving As_2O_3(s) in 1 mol/L NaOH. The $NaNO_3$ used to adjust the ionic strength was obtained from Fisher Scientific. All solutions were prepared with deionized water (18 MΩ-cm) prepared using a Hydro-Service reverse osmosis/ion exchange apparatus (Model LPRO-20).

Preparation of iron-coated sand and manganese-coated sand

Initially, $Mn(NO_3)_2$ solution (100 mL of 0.1 mol/L), previously adjusted to pH 8 with NaOH solution, was mixed with Joomoonjin sand (100 g) in a rotary evaporator. By rotating the rotary evaporator at 30 rpm in a water bath maintained at 70–80 °C, water was continuously removed from the suspension of manganese and sand by applying a vacuum until approximately 10% of water remained in the suspension. Thereafter, the sand was dried at three different temperatures, i.e. 150, 300 and 600 °C, for 1 h. In order to remove the trace of uncoated manganese, the dried sand was rinsed several times with distilled water and then dried again at 105 °C. In the preparation of ICS, $FeCl_3$ solution (100 mL of 0.1 mol/L), previously adjusted to pH 12 with NaOH solution, was mixed with Joomoonjin sand (100 g) in a rotary evaporator. The same procedure used in the preparation of MCS was then followed. Manganese and iron coated on the sand were stripped using an acid digestion method (U.S.EPA 3050B). After filtration, the dissolved concentrations of manganese and iron were measured using an inductively coupled plasma (ICP, model Optima 2000 DV, Perkin Elmer Co.). The mineral types of the ICS and MCS were characterized by X-ray diffraction (XRD, model D/MAX, Rigaku). Photomicrography and inorganic contents of the Joomoonjin sand, ICS and MCS, were obtained by Scanning Electron Micrograph-Energy Dispersive Spectroscopy (SEM-EDX, model JSM-5900, JEOL). The Brunauer–Emmett–Teller (BET) surface areas, porosities and pore sizes of the Joomoonjin sand, ICS and MCS were determined using a computer-controlled nitrogen gas adsorption analyzer.

Batch adsorption and oxidation

In order to study the effects of coating temperature on As(V) adsorption, each ICS (20 g/L) was mixed with 4 mg/L of As(V) in plastic bottles. All experiments were conducted at a fixed ionic strength (0.01 mol/L $NaNO_3$) and ambient temperature (22–25 °C). The initial pH of the suspensions was adjusted to 4.5 using 0.01 mol/L HNO_3 and 0.01 mol/L NaOH. The plastic bottles were shaken for at least 24 h to ensure sufficient reaction time. The pH of each suspension was measured at constant time intervals and adjusted to 4.5 up to the equilibration time. After the reaction, the suspension was filtered through 0.45-μm syringe filters. The total dissolved arsenic concentration in the filtrate was measured using ICP. The adsorbed arsenic concentration was calculated from the difference between the total initial arsenic concentration and the total dissolved arsenic concentration.

In order to investigate the effect of coating temperature on the As(III) oxidation, each MCS (20 g/L) was mixed with 10 mg/L of As(III) in plastic bottles. The other experimental conditions were the same as those in the As(V) adsorption. A portion of the sample was then subjected to a modified anion exchange method (Vaishya & Gupta 2002) to quantify the As(III) and As(V). The chloride form of the anion-exchange resin (Dowex 1×8–100, sigma) was converted to the acetate form in a glass-column ($d = 0.8$ cm, 1.5 mL resin). Prior to the separation of As(III) and As(V), the pH of each sample was adjusted to around 3.5. Under this conditions, the fully protonated As(III) passes through the column, while the partially deprotonated As(V) was retained. The total dissolved arsenic concentrations before and after the column test were measured using ICP. The As(V) concentration was then calculated by difference and used to calculate the As(III) oxidation efficiency in aqueous solution. FT-IR spectra of ICS after the As(V) adsorption test were obtained using an FT-IR spectrophotometer (Mattson 1000 FT-IR, England). The dry sample (about 0.1 g) was mixed with KBr (0.1 g) and pressed into tablet form.

RESULTS AND DISCUSSION

Characterization of ICS and MCS

Figure 1 shows that the amounts of iron and manganese coated onto the sand were reasonably constant irrespective of the coating temperatures in the preparation of both ICS and MCS. The SEM images of acid-washed natural Joomoonjin sand in Figure 2(a) show a relatively uniform and smooth surface. The ICS samples (Figures 2(b)–(d)) had significantly rougher surfaces than the Joomoonjin sand. Crystal growth was observed on the surface of ICS and MCS prepared above 300 °C compared with that of ICS-150 and MCS-150 prepared at 150 °C (Figure 3). The measured surface areas of the Joomoonjin sand, ICS and MCS prepared at all temperatures were below 1.5 m^2/g, as shown in Table 1 (Figure 3).

As the composition of Si in the ICS and MCS was approximately 45%, as assessed from the EDX measurements, it was difficult to clearly determine the mineral type. Thus, the powders obtained from the same procedures for the preparation of ICS and MCS without the presence of Joomoonjin sand were used to analyze the mineral type. Figure 4(a) and (b) shows the X-ray diffraction spectra of iron and manganese oxides, respectively, using Cu$_{K\alpha}$

Table 1 | Specific surface areas of raw sand, ICS and MCS prepared at different coating temperatures

| Raw sand | Sample | Coating temperature | | |
		150 °C	300 °C	600 °C
0.36 m^2/g	ICS (m^2/g)	1.45	1.00	0.86
	MCS (m^2/g)	0.74	0.72	0.84

radiation ($\lambda = 1.5406$ Å) at kV = 40 and mA = 100, with a scan speed = 2.4 θ/min and scan range = 10 ~ 80 θ. The mineral type of ICS-150 was identified as a mixture of goethite (α-FeOOH) and hematite (α-Fe$_2$O$_3$), but this chemical was changed to high crystalline goethite above 300 °C due to a hydrothermal reaction. The mineral type of iron oxide on the ICS is known to depend on the coating temperature (Lo *et al.* 1997). From the coating of Fe(III) on the silica, Lo *et al.* (1997) reported coating of Fe(III) as amorphous iron oxides at 60 °C, as a mixture of goethite and hematite at 150 °C and as hematite above 300 °C.

The mineral type of MCS-150, prepared at 150 °C, was identified as a mixture of pyrolusite (β-MnO$_2$) and ramsdellite (γ-MnO$_2$, a mixture of α-MnO$_2$ and β-MnO$_2$), as shown in Figure 4, while it also changed to high crystalline β-MnO$_2$ above 300 °C due to a hydrothermal reaction.

Batch adsorption

Figure 5 shows that the adsorption of As(V) onto the ICS was greatly decreased with increasing coating temperature. The amount of As(V) adsorbed onto the ICS-600 was approximately 30% of that of the ICS-150. As shown in Figure 1, the amounts of Fe(III) coated were similar for all the ICS samples, although they were prepared at different temperatures. Therefore, the different As(V) adsorption efficiencies by ICS prepared at different temperatures can be explained by the different physicochemical properties of the coated Fe(III), such as surface area and mineral type, etc. The specific surface area of the ICS prepared at three different coating temperatures ranged from 0.864 to
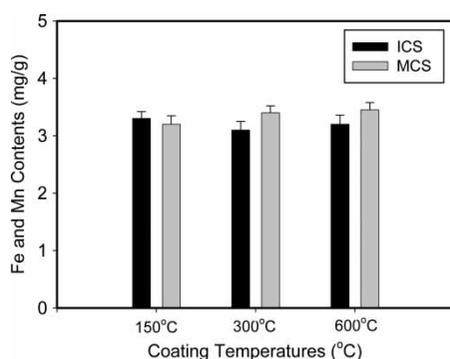

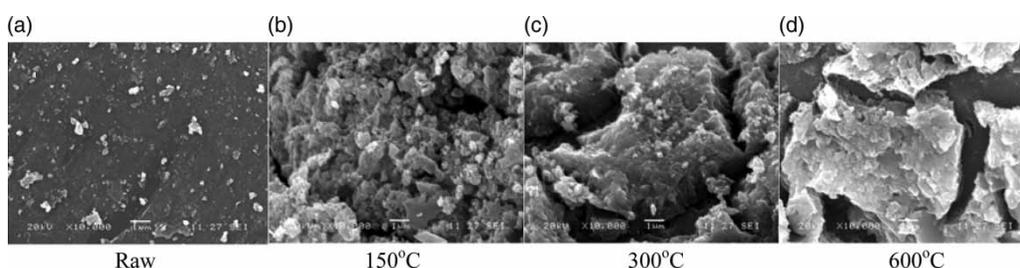**Figure 1** | The Fe and Mn contents on ICS and MCS prepared at different coating temperatures.

Figure 2 | SEM images (×10,000) of ICS prepared at different coating temperatures. (a) Raw (b) 150 °C (c) 300 °C (d) 600 °C.
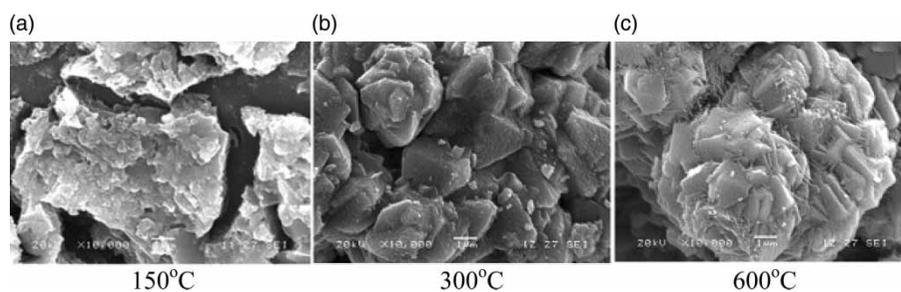
Figure 3 | SEM images (×10,000) of MCS prepared at different coating temperatures. (a) 150 °C (b) 300 °C (c) 600 °C.
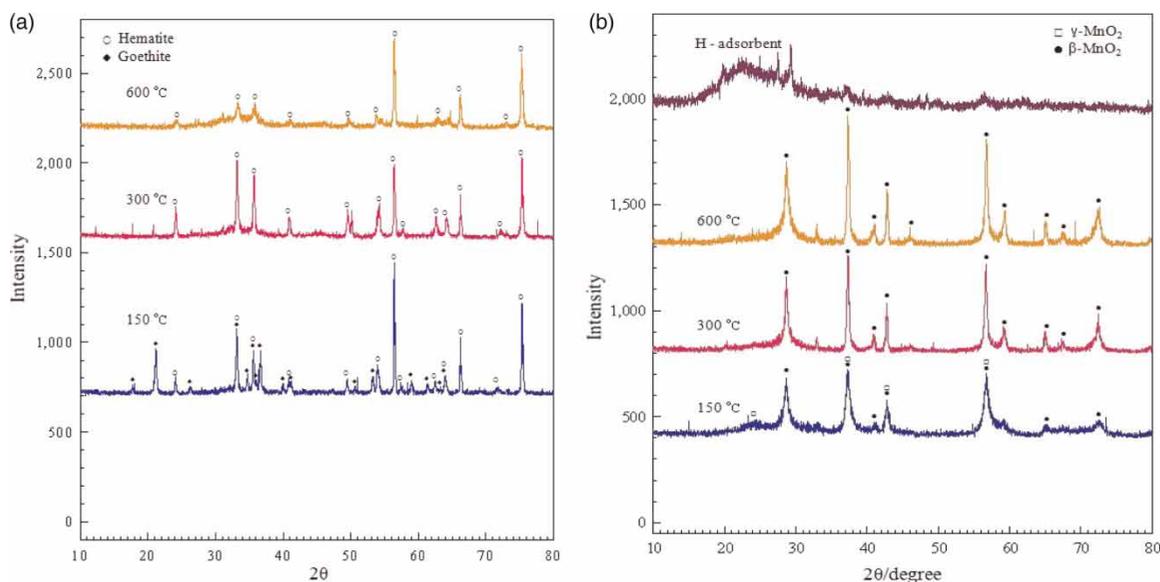

Figure 4 | XRD patterns of (a) ICS and (b) MCS prepared at different coating temperatures.
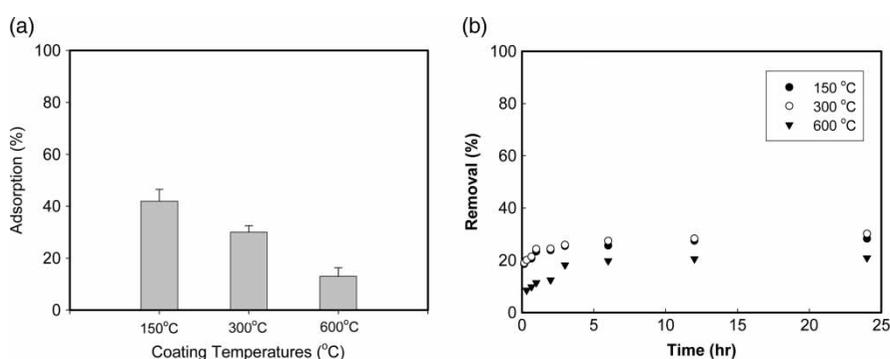

Figure 5 | Adsorptions of As(V) by ICS prepared at different coating temperatures (a) at various times and (b) (pH = 4.5, initial As(V) = 4 ppm, ionic strength = 0.01 mol/L NaNO₃, ICS dosage = 0.5 g).

1.448 m²/g. Ohe *et al.* (2010) reported that adsorption capacities of both As(III) and As(V) onto magnetite increased with increasing specific surface area. In addition, the mineral type is regarded as the other important factor affecting the different adsorption efficiencies of the ICS.

The mineral type of ICS-150 was identified as a mixture of goethite and hematite, but this compound changed to high crystalline goethite at 300 and 600 °C, From the adsorption isotherm experiments of As(III) and As(V) onto natural hematite, goethite and magnetite, Giménez *et al.* (2007)
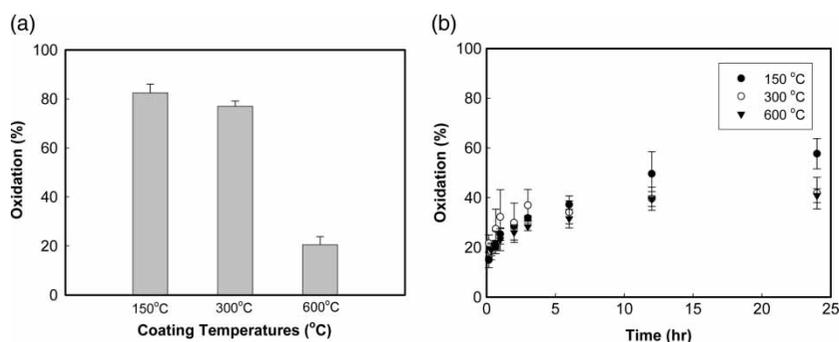
Figure 6 │ Oxidations of As(III) by MCS prepared at different coating temperatures (pH = 4.5, initial As(III) = 10 ppm, ionic strength = 0.01 mol/L $NaNO_3$, MCS dosage = 0.5 g).

reported that both As(III) and As(V) were efficiently sorbed onto hematite rather than goethite or magnetite. This result supports that adsorption of arsenic onto metal oxides can be controlled by the mineral types as well as surface area.

Batch oxidation

Figure 6 shows that the oxidation efficiency of As(III) by the MCS was similar up to a coating temperature of 300 °C, but greatly decreased oxidation efficiency was observed with MCS-600. As shown in Figure 1, the amounts of Mn coated on the sand substrate were similar for all the MCS samples, even though they were prepared at different temperatures. Therefore, the different As(III) oxidation efficiencies by MCS prepared at different coating temperatures can also be explained by the different mineral types of the manganese oxide coated. The mineral type of MCS-150 was identified as a mixture of the pyrolusite and ramsdellite, but was also changed to high crystalline β-MnO_2 above 300 °C, as discussed previously. Hu et al. (2004) reported that manganese-coated sand prepared under moderate temperature and acidic conditions during the impregnation processes with igneous rock and $KMnO_4$ had a mixture of mineral types, such as pyrolusite, γ-Mn_2O_3 and $Mn(OH)_4$.

Adsorption mechanism of As(V) onto the ICS

Figure 7 shows the FT-IR spectrum of the ICS-150 obtained after arsenic adsorption. The FT-IR spectrum shows peaks at 806 and at 890 cm^{-1}, corresponding to As–O–Fe vibration resulting from the adsorption of As(V) onto goethite and to As–O–Fe vibration resulting from the adsorption of As(V) onto hematite, respectively. Muller et al. (2010) reported that the peaks observed within the wavelength bands 806–817 and 854–861 cm^{-1} originated from the vibration of Fe–O–As groups and the vibration of a non-complexed
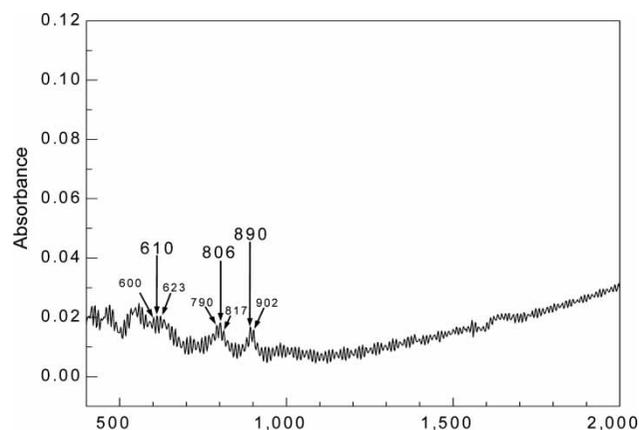

Figure 7 │ FT-IR spectrum of ICS prepared at 150 °C.

As–O bond. Also, Williams & Scherer (2004) observed that the As(V) adsorbed onto the surface of hematite showed a peak at 890 cm^{-1}. From the XRD measurement, the mineral type of the ICS-150 was identified as a mixture of goethite and hematite. Therefore, the spectroscopic result was well matched with XRD measurement. These results may suggest that As(V) removal by ICS occurs through the surface complex between the iron on the surface of ICS and As(V).

CONCLUSIONS

From this research, the mineral types of iron and manganese coated onto the surface of the ICS and MCS changed with variation of the coating temperature. High crystalline goethite and β-MnO_2 developed on the surface of ICS and MCS, respectively, and prepared above 300 °C showed much lower As(V) adsorption and As(III) oxidation efficiencies. Considering the growth of high crystalline goethite and β-MnO_2 above 300 °C and the formation of a surface complex between As(V) and Fe(III) on the surface of ICS

prepared at 150 °C, ICS and MCS that were prepared at 150 °C were identified as good materials for the removal of As(III) through the promising oxidation efficiency of As (III) to As(V) by MCS and the adsorption of As(V) by both the MCS and ICS.

ACKNOWLEDGEMENTS

REFERENCES

Ali, I. & Gupta, V. K. 2007 Advances in water treatment by adsorption technology. *Nature Protocols* **1**, 2661–2667.

Chang, Y. Y., Kim, K. S., Jung, J. H., Yang, J. K. & Lee, S. M. 2007 Application of iron-coated sand and manganese-coated sand on the treatment of both As(III) and As(V). *Water Sci. Technol.* **55**, 69–75.

Chang, Y. Y., Song, K. H. & Yang, J. K. 2008 Removal of As(III) in a column reactor packed with iron-coated sand and manganese-coated sand. *J. Hazard Mater.* **150**, 565–572.

Chen, H. W., Frey, M. M., Clifford, D., McNeill, L. S. & Edwards, M. 1999 Arsenic treatment considerations. *J. Amer. Water Works Assoc.* **91**, 74–85.

Giménez, J., Martínez, M., Pablo, J., Rovira, M. & Duro, L. 2007 Arsenic sorption onto natural hematite, magnetite, and goethite. *J. Hazard Mater.* **141**, 575–580.

Gupta, V. K. & Ali, I. 2008 Removal of endosulfan and methoxychlor from water on carbon slurry. *Environ. Sci. Technol.* **42**, 766–770.

Gupta, V. K. & Rastogi, A. 2008a Biosorption of lead(II) from aqueous solutions by nonliving algal biomass *Oedogonium* sp. and *Nostoc* sp. – a comparative study. *Coll. & Surfaces B* **64** (2), 170–178.

Gupta, V. K. & Rastogi, A. 2008b Equilibrium and kinetic modeling of cadmium (II) biosorption by nonliving algal biomass *Oedogonium* sp. from aqueous phase. *J. Hazard Mater.* **153** (1–2), 759–766.

Gupta, V. K. & Sharma, S. 2002 Removal of cadmium and zinc from aqueous solutions using red mud. *Environ. Sci. Technol.* **36**, 3612–3617.

Gupta, V. K., Rastogi, A., Dwivedi, M. K. & Mohan, D. 1997a Process development for the removal of zinc and cadmium from wastewater using slag – A blast furnace waste material. *Sep. Sci. Technol.* **32**, 2883–2912.

Gupta, V. K., Srivastava, S. K., Mohan, D. & Sharma, S. 1997b Design parameters for fixed bed reactors of activated carbon developed from fertilizer waste material for the removal of some heavy metal ions. *Waste Manage.* **17**, 517–522.

Gupta, V. K., Mohan, D. & Sharma, S. 1998 Removal of lead from wastewater using bagasse fly ash-a sugar industry waste material. *Sep. Sci. Technol.* **33** (9), 1331–1343.

Gupta, V. K., Saini, V. K. & Jain, N. 2005 Adsorption of As(III) from aqueous solutions by iron-oxide coated sand. *J. Colloid Interface Sci.* **288**, 55–60.

Gupta, V. K., Carrott, P. J. M., Ribeiro, M. M. L. & Suhas, T. I. 2009 Low cost adsorbents: growing approach to wastewater treatment – a review. *Critical Rev. Environ. Sci. Technol.* **39**, 783–842.

Gupta, V. K., Rastogi, A. & Nayak, A. 2010 Adsorption studies on the removal of hexavalent chromium from aqueous solution using a low cost fertilizer industry waste material. *J. Colloid Interface Sci.* **342**, 135–141.

Hu, P. Y., Hsieh, Y. H., Chen, J. C. & Chang, C. Y. 2004 Characteristics of manganese-coated sand using SEM and EDAX analysis. *J. Colloid Interface Sci.* **272**, 308–318.

Kim, M. J., Nriagu, J. & Haack, S. 2002 Arsenic species and chemistry in groundwater of southeast Michigan. *Environ. Pollut.* **120**, 379–390.

Lo, S. L., Jeng, H. T. & Lai, C. H. 1997 Characteristics and adsorption properties of iron-coated sand. *Water Sci. Technol.* **35**, 63–70.

Muller, K., Ciminell, V. S. T. & Willscher, S. 2010 A comparative study of As(III) and As(V) in aqueous solutions and adsorbed on iron oxy-hydroxides by Raman spectroscopy. *Water Res.* **44**, 5660–5672.

Ohe, K., Oshima, T. & Baba, Y. 2010 Adsorption of arsenic using high surface area magnetites. *Environ. Geochem. Health* **32**, 283–286.

Smedley, P. L. & Kinniburgh, D. G. 2002 A review of the source, behaviour and distribution of arsenic in natural waters. *Appl. Geochem.* **17**, 517–568.

Srivastava, S. K., Gupta, V. K. & Mohan, D. 1997 Removal of lead and chromium by activated slag – A blast-furnace waste, *J. Envorn. Engng. (ASCE)* **123**, 461–468.

Vaishya, R. C. & Gupta, S. K. 2002 Modelling arsenic(III) adsorption from water by sulfate-modified iron oxide-coated sand (SMIOCS). *J. Chem. Technol. Biotechnol.* **78**, 73–80.

Williams, A. G. B. & Scherer, M. M. 2004 Spectroscopic evidence for Fe(II)-Fe(III) electron transfer at the iron oxide-water interface. *Environ. Sci. Technol.* **38**, 4782–4790.

Yang, J. K., Song, K. H., Kim, B. K., Hong, S. C., Cho, D. E. & Chang, Y. Y. 2007 Arsenic removal by iron and manganese coated sand. *Water Sci. Technol.* **56**, 161–169.

Zhang, F. S. & Itoh, H. 2005 Iron-oxide loaded slag for arsenic removal from aqueous system. *Chemosphere* **60**, 319–325.